Long-lived anticyclonic eddies facilitate convection in the Greenland Sea over multiple consecutive winters

Dong Jian[1], Xiaoming Zhai[1], Ian A. Renfrew[1], David P. Stevens[2]

[1]School of Environmental Sciences, University of East Anglia, Norwich, United Kingdom
[2]School of Engineering, Mathematics and Physics, University of East Anglia, Norwich, United Kingdom

Key Points:

- A previously undiscovered long-lived anticyclonic eddy in the Boreas Basin is identified from observations and model simulations
- Long-lived anticyclonic eddies act to confine and facilitate open ocean deep convection
- Long-lived anticyclonic eddies facilitate convection over several consecutive years

Corresponding author: Dong Jian, d.jian@uea.ac.uk

Abstract

Wintertime open-ocean convection is a key process in renewing deep water; however, the processes that promote convection on local scale remain poorly understood. We investigate the role of long-lived anticyclonic eddies in facilitating deep convection in the Greenland Sea using a new model simulation and observations. We find a previously undocumented anticyclonic eddy in the Boreas Basin, in addition to a well-observed anticyclonic eddy in the Greenland Basin. Both eddies feature year-round lenses of weak stratification with upper-domed isopycnals, facilitating convection over multiple winters.

Plain Language Summary

Open-ocean convection in the Greenland Sea plays a key role in water-mass transformation within the global ocean. These convective events occur at many scales, but are often observed within deep, well-mixed "chimneys" or as rotating structures (eddies). Using a high-resolution ocean model, we successfully reproduce these features and show that long-lived anticyclonic eddies in the Greenland Sea favor convection over multiple consecutive winters.

1 Introduction

The Greenland Sea (Figure 1) is characterized by a cyclonic gyre composed primarily of the southward East Greenland Current (EGC) and the northward Norwegian Atlantic Front Current (NAFC). Pronounced recirculations and meanders form two subgyres separated by the Greenland Fracture Zone, which divides the Boreas and Greenland Basins (Quadfasel & Meincke, 1987). Owing to the cyclonic circulation and wintertime air-sea heat loss, this is one of the few regions globally where open-ocean convection occurs, renewing intermediate and deep waters (Marshall & Schott, 1999).

Observations in the Greenland Sea show that intermittent bottom-reaching convection has transitioned to predominantly intermediate-depth convection since the late 20th century (Strehl et al., 2024). Since then, attention has focused on long-lived vortices with convective signatures in the Greenland Basin, notably the 75°N eddy repeatedly detected near 75°N, 0°E during ship-based surveys in the 2000s (Gascard et al., 2002; Wadhams, 2005; Budéus & Ronski, 2009). In March 2001, observations revealed a homogeneous eddy core extending to $\sim$ 1800 m, characterized by colder and fresher water relative to the surrounding basin (Wadhams et al., 2002). Surveys in 1997, 2001, and 2002 reported a distinct anticyclonic vortex at the same location, indicating a long-lived feature.

Argo profiles provide evidence that intermediate-to-deep convection occurred in 2002, 2008, and 2011 (Brakstad et al., 2019; Almeida et al., 2023) and confirm a secondary maximum of mixed-layer depth within the Boreas Basin, northern Greenland Sea, although profiling coverage there is sparser (Brakstad et al., 2019; Abot et al., 2023). Whether the convective eddies play a role in recent convection events is uncertain. Using a high-resolution model and observations, we revisit the structure, evolution, and dynamical role of long-lived anticyclonic eddies with convective features in the Greenland Sea. The model successfully reproduces the 75°N eddy in the Greenland Basin and, unexpectedly, reveals a comparable convective structure in the Boreas Basin, corroborated by observations. This study thus provides an updated perspective on eddy-convection relations in the region.

2 Data and Methods

2.1 Observations

During March–April 2008, two surface drifters traversed the Greenland Sea; six Argo floats were in the Greenland Basin, and one was in the Boreas Basin, yielding 41 valid profiles over 2 months. Combining these profiles with drifter trajectories and altimetry-derived surface geostrophic velocity, we identify two representative Argo casts exhibiting convective signatures associated with eddies. In addition, recent 2-km resolution SWOT altimetry provides further context.

2.2 Model

We use a very high-resolution hydrostatic ocean–ice model MITgcm (Marshall et al., 1997), configured and validated for the Nordic Seas. The Greenland Sea region has a 1.5-2 km horizontal resolution, which is significantly finer than the local first Rossby radius of 4.7 km (Nurser & Bacon, 2014). The model is initialized with GLORYS ocean reanalysis fields and forced by ERA5 atmospheric forcing from 1993 onward. Model configuration and validation are described in Jian et al. (2026). The K-Profile Parameterization represents unresolved processes in vertical mixing (Large et al., 1994). Comparisons of simulated sea ice extent, circulation, and mixed-layer depth with observations demonstrate its accuracy (Figures 1-2). Long-lived anticyclonic eddy centers are tracked by identifying local minima of negative relative vorticity at 1500 m every five days, with constraints imposed by topographic depressions and temporal continuity of eddy displacement. Eddy tracking is further verified by visual inspection (Figure S1).

2.3 Diagnostics

The mixed-layer depth (MLD) is defined as the depth where potential density increases relative to 10 m depth by an equivalent 0.2 °C cooling (Våge et al., 2015; Brakstad et al., 2023). The buoyancy (Brunt–Väisälä) frequency squared, N^2, a measure of vertical stratification, is calculated using the TEOS-10 Gibbs SeaWater equations of state (IOC et al., 2010). Large N^2 indicates strong stratification, while small or near-zero N^2 indicates weak static stability and susceptibility to vertical mixing (Våge et al., 2009; Talley, 2011).

3 Results

3.1 Basin-scale context

Multiple observations in March-April 2008 provide evidence that deep convection occurred across the Greenland Sea (Figure 1a). The observed sea-ice edge was aligned with the shelf and remained distant from the open ocean, allowing sustained surface cooling. Two surface drifters traversed the Greenland Sea from northeast to southwest, illustrating the cyclonic surface circulation and decreasing surface temperature en route. Temperatures declined from ∼1 °C in the Boreas Basin during March to below 0 °C in the Greenland Basin by April, reflecting both air–sea heat loss and advection into colder waters in the Greenland Basin, promoted by northerly winds. Several looping and meandering mesoscale to submesoscale features are evident. The MLD calculated from Argo profiles captures deep convection in the central Greenland Basin as well as a secondary convection site in the Boreas Basin. Two representative Argo profiles capture the near-homogeneous water columns of April 2008 near anticyclonic eddies in the Boreas and central Greenland basins, evident in altimetry-derived geostrophic velocity maps (Figure 1c). The Boreas Basin profile collected on April 3rd exhibits a uniform temperature down to 600 m, with thermal stratification below; concurrent altimetry indicates that the float was positioned near an anticyclonic eddy rim (Figure 1c). The Greenland Basin profile

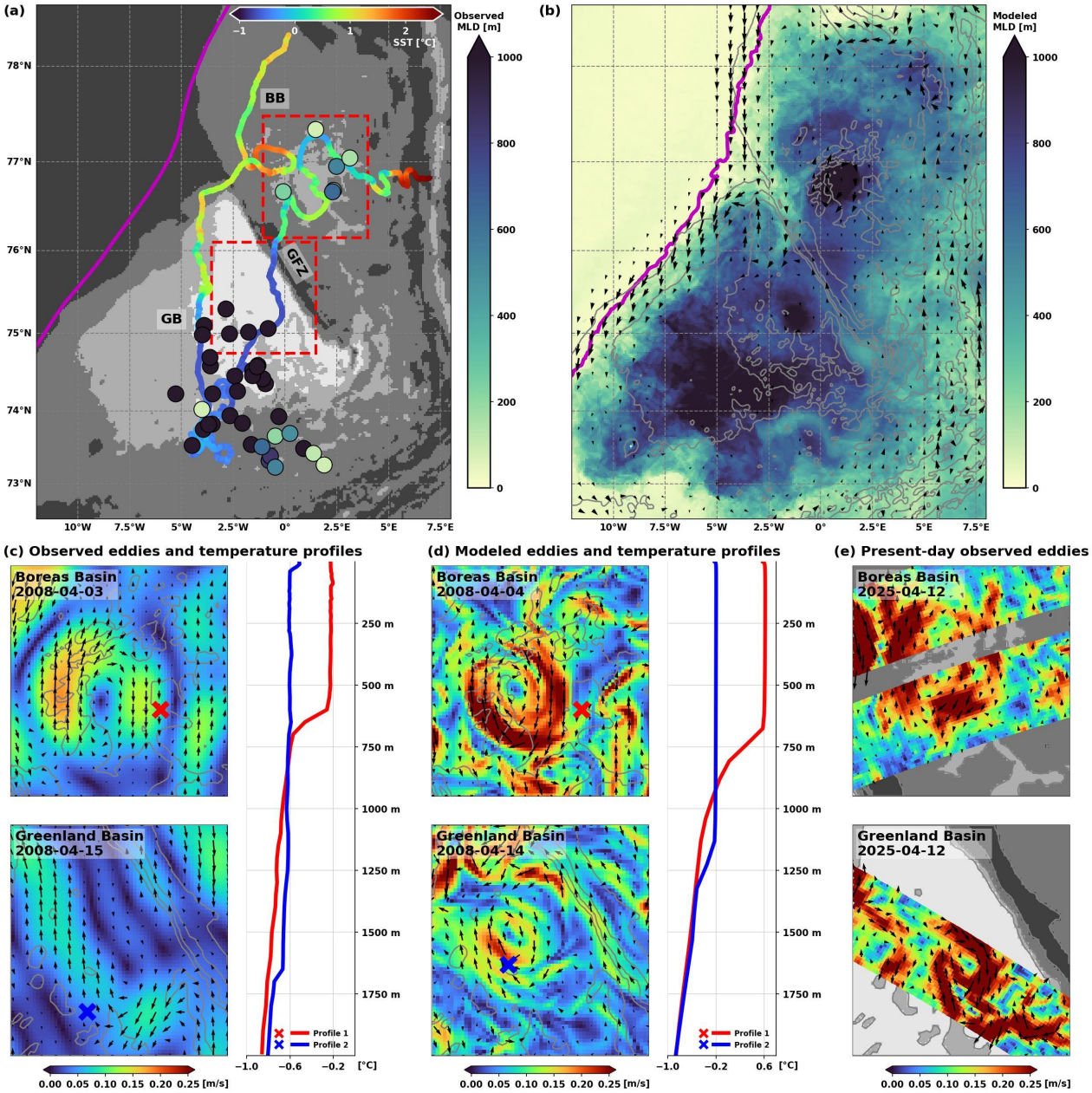

Figure 1. (a) Observed and (b) modeled mixed-layer depth (MLD) in the Greenland Sea during March–April 2008. The presence of eddies in two topographic depressions from (c) altimeter-based, (d) model-based, and (e) SWOT-based surface geostrophic velocity. In (a), dots denote Argo-derived MLD, trajectories show drifter-recorded sea surface temperature, and magenta line is observed mean 75% sea-ice extent during March–April 2008. Panel (b) shows modeled time-mean MLD, surface geostrophic circulation, and 75% sea-ice extent for the same period. Red boxes highlight topographic depressions where long-lived eddies reside and correspond to the maps in (c-e). Two observed Argo profiles in (c) are compared to modeled profiles in (d), with cast locations (x) and dates denoted in the maps showing surface geostrophic velocities. Acronyms denote the Boreas Basin (BB), Greenland Fracture Zone (GFZ), and Greenland Basin (GB). The 2400, 3200, and 3600 m isobaths in maps are shown throughout the paper.

collected on April 15th near 75°N shows a deeper mixed layer of $\sim$ 1700 m, in proximity to a smaller anticyclonic eddy. Although conventional altimetry cannot reliably resolve the smallest eddies in the central Greenland Basin, anticyclonic eddies with convective signatures near 75°N have been frequently documented in historical ship-based surveys (Wadhams, 2005; Budéus & Ronski, 2009).

The modeled surface geostrophic circulation agrees well with established schematics (Quadfasel & Meincke, 1987), reproducing the cyclonic gyre that favors deep convection and capturing a realistic sea-ice extent (Figure 1b). The model simulates deep mixed layers across the Greenland Basin and a secondary maximum in the Boreas Basin, consistent with observations. Two distinct anticyclonic eddies, one in the Boreas Basin and another near 75°N in the Greenland Basin, occupy topographic depressions and coincide with the mesoscale swirls observed in the drifter trajectories. The simulated hydrographic profiles near the eddy rim and at the nearest profiling date are comparable to those observed (Figure 1d). The model exhibits a +0.5 °C temperature bias in both regions and a shallower convective depth in the central Greenland Basin compared to the Argo profiles. Yet, it captures the key features: the homogeneous water column, location, timing, rotation, spatial scales, and convective characteristics of both eddies.

Additionally, SAR data, MODIS imagery, and SWOT altimetry (Figure 1e) reveal recurrent eddies at similar locations, with frequent merging events (Bashmachnikov et al., 2020; Morozov & Kozlov, 2023; Jensen et al., 2025). The observed eddies exhibit spatial scales comparable to those simulated in the model. Together, these observations and model simulations identify two anticyclonic eddies in topographic depressions with wintertime convective features. The Boreas Basin eddy has not been documented before. We hereafter refer to the two as the BB eddy and the 75°N eddy, and probe their interactions with convection using model simulations.

3.2 Evolution of eddies and convection

Monthly-mean surface geostrophic circulation from altimeter and model, together with the modeled isopycnal depth and MLD from January to May 2008 illustrate the progression of convection (Figure 2). The model reproduces the cyclonic gyre in agreement with altimetry-derived circulation and additionally represents mesoscale eddies that the altimeter may not reliably resolve. While the BB eddy, evident in both products, remains quasi-stationary and topographically constrained, the modeled 75°N eddy is embedded within the broader basin-wide convective region and drifts northwestward from April onward, likely guided by local topography (Figure 1a). Gyre-scale cyclonic circulation pushes the dense 28.04 $\mathrm{kg\,m^{-3}}$ isopycnal closer to the surface in the gyre center. Surface outcrops of this isopycnal (Figure 2c) gradually emerge as winter progresses, primarily in the Greenland Basin and in isolation within the BB eddy. In both eddies, the 28.04 $\mathrm{kg\,m^{-3}}$ isopycnal outcrops in March at the eddy centers, indicating convection occurring within the eddies. The deepest mixed layers are found within two eddies and more broadly across the Greenland Basin. By May, the mixed layer shoals, and the surface isopycnal outcrops subside, marking the cessation of active convection and the onset of restratification. This pattern is consistent with climatological MLD maps derived from hydrographic observations (Brakstad et al., 2019, 2023) and demonstrates that eddy-related mixing is an integral component of basin-scale convection.

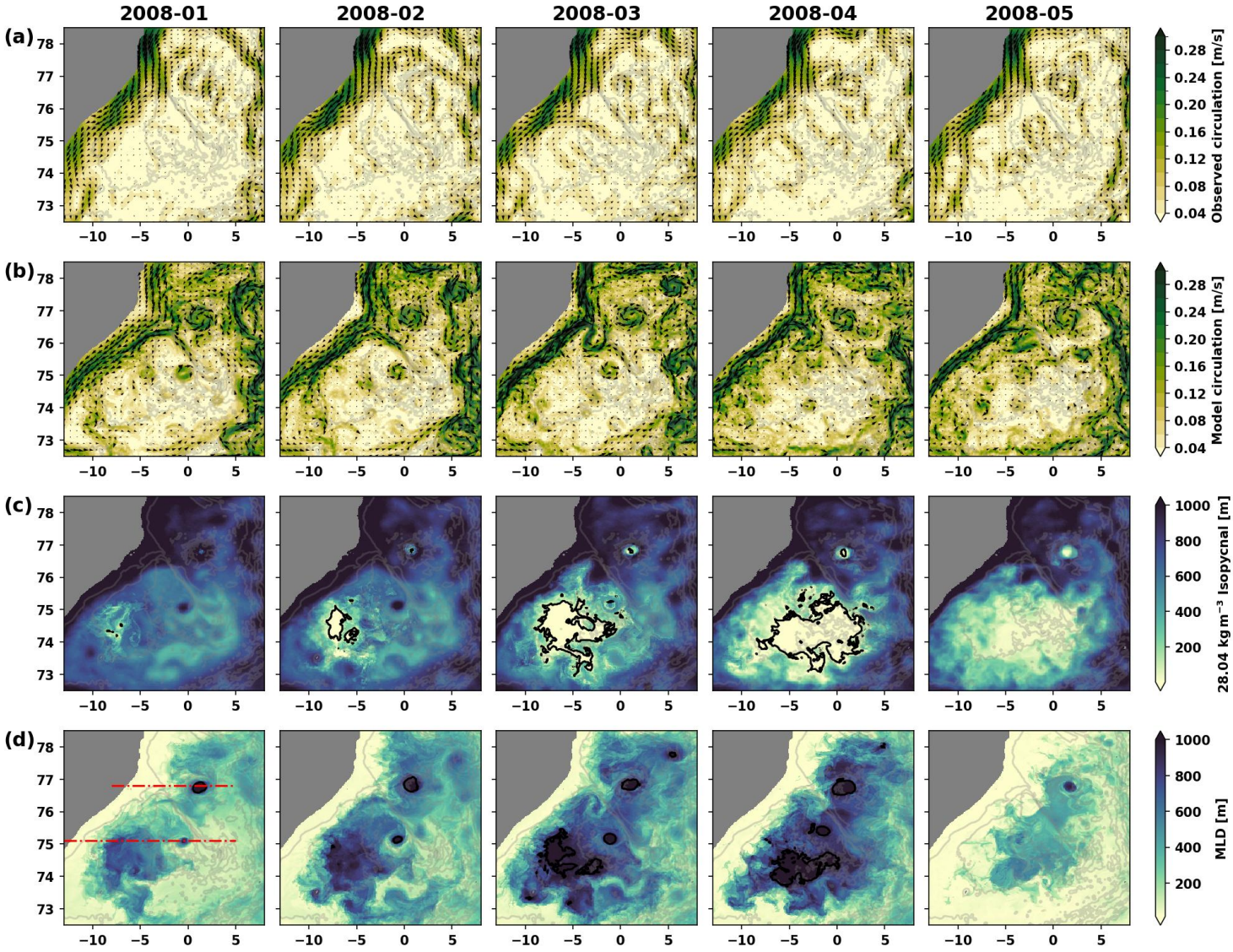

Figure 2. Monthly-mean surface geostrophic circulation from (a) altimeter-based gridded product and (b) model, plus (c) depth of the 28.04 $\mathrm{kg\,m^{-3}}$ isopycnal, and (d) mixed-layer depth (MLD) from the model for January to May, 2008. Black contours in panel (c) denote 28.04 $\mathrm{kg\,m^{-3}}$ isopycnal surface outcrops, and in panel (d) denote 1000 m MLD. Two red lines in panel (d) denote zonal transects described in the following section. East Greenland Shelf shallower than 1000 m is masked.

3.2.1 Boreas Basin Eddy

Modeled zonal transects across the BB eddy center from five representative stages illustrate the evolution of convective mixing within this anticyclonic eddy (Figure 3). The stage selection is made by identifying the time of maximum MLD and choosing two representative frames before and after.

Initial (column 1): On November 1st, 2007, the five-day mean net surface heat loss along the latitude across the BB eddy center remains weak. Modeled hydrography crossing the EGC exhibits a three-layered structure consistent with ship-surveyed observations (Håvik et al., 2017): cold, fresh Polar Surface Water at the surface; Atlantic-origin water beneath that shoals offshore, comprising warm returning Atlantic Water and colder, less saline Arctic Atlantic Water banked against the slope; and a deeper, colder, dense layer. Far offshore, away from any ship-based surveys, is a rapidly rotating anticyclonic eddy with distinct water masses centered near 1000 m depth. Isopycnals remain stratified but exhibit gentle doming within the anticyclonic eddy core, with lighter 28.03 and 28.04 kg m^{-3} isopycnal surfaces uplifted and denser ones displaced downward. The N^2 is high throughout most of the water column, except in the surface layer directly contacting the atmosphere and within the weakly stratified, warm, saline eddy core.

Onset (column 2): By mid-February, southward advection of Polar Surface Water and sustained surface heat loss progressively cool the upper ocean and erode stratification. The net surface heat loss averages 200–300 W/m^2 over the previous 3.5 months. The 1°C isotherm outcrops to form a cylindrical structure in the upper eddy, while the 0.5°C isotherm uplifts from the base of the eddy, establishing a convective lens ("chimney") that renders the eddy nearly vertically homogeneous in temperature and salinity and enclosed by ambient waters. The 28.03 and 28.04 kg m^{-3} isopycnals outcrop within the eddy center, with isopycnals tilting downward on the left flank and upward on the right flank, favoring convection within the eddy and farther offshore. The N^2 is very low throughout the eddy and in the surrounding surface layer where denser isopycnals are uplifted. This weakly stratified region delineates the deepening mixed layer, indicating vigorous vertical mixing that occurs preferentially within the eddy.

Peak (column 3): On April 4th, the mixed-layer reaches its maximum depth and widest spatial extent, marking the peak phase of convection. While episodes of extreme heat loss of up to 800 W/m^2 occur near the ice edge, the eddy ∼150 km to the east experiences more moderate forcing (∼300 W/m^2). Despite this, the eddy interior becomes progressively colder and fresher, in concert with the surrounding upper ocean. The 0.5, 0.3 °C isotherms, the 34.94, 34.93 isohalines, and the 28.03 to 28.05 kg m^{-3} isopycnals all outcrop, while the downward-sloping 28.06 kg m^{-3} isopycnal in the eddy base resists further vertical mixing. The upper ∼700 m surrounding the eddy is statically unstable, whereas the instability within the eddy itself, as indicated by N^2, extends to depths of ∼ 1500 m. Near the eddy rim, the upper water column is also vertically homogeneous to a limited depth, underlain by a pronounced thermocline and halocline. This vertical hydrographic structure closely resembles the Argo temperature profile sampled on April 3rd and is well reproduced by the model (Figure 1c,d). Note the rapid anticyclonic rotation likely deflects Argo floats away from the eddy interior, causing floats to preferentially sample the rim rather than the center, where the deepest convection occurs and direct measurements are scarce.

Halt (column 4): By late May, surface heat fluxes weaken and reverse sign; open-ocean convection ceases, and the restratification of the upper ocean starts, along with the breakdown of the upper cylindrical convective lens. The eddy becomes capped by a warm, saline surface layer, while its upper-domed isopycnals persist beneath. The eddy core remains sandwiched between stratified layers above and below, with weakly buoyant ambient water spreading laterally and residing near 500 m depth as a convective

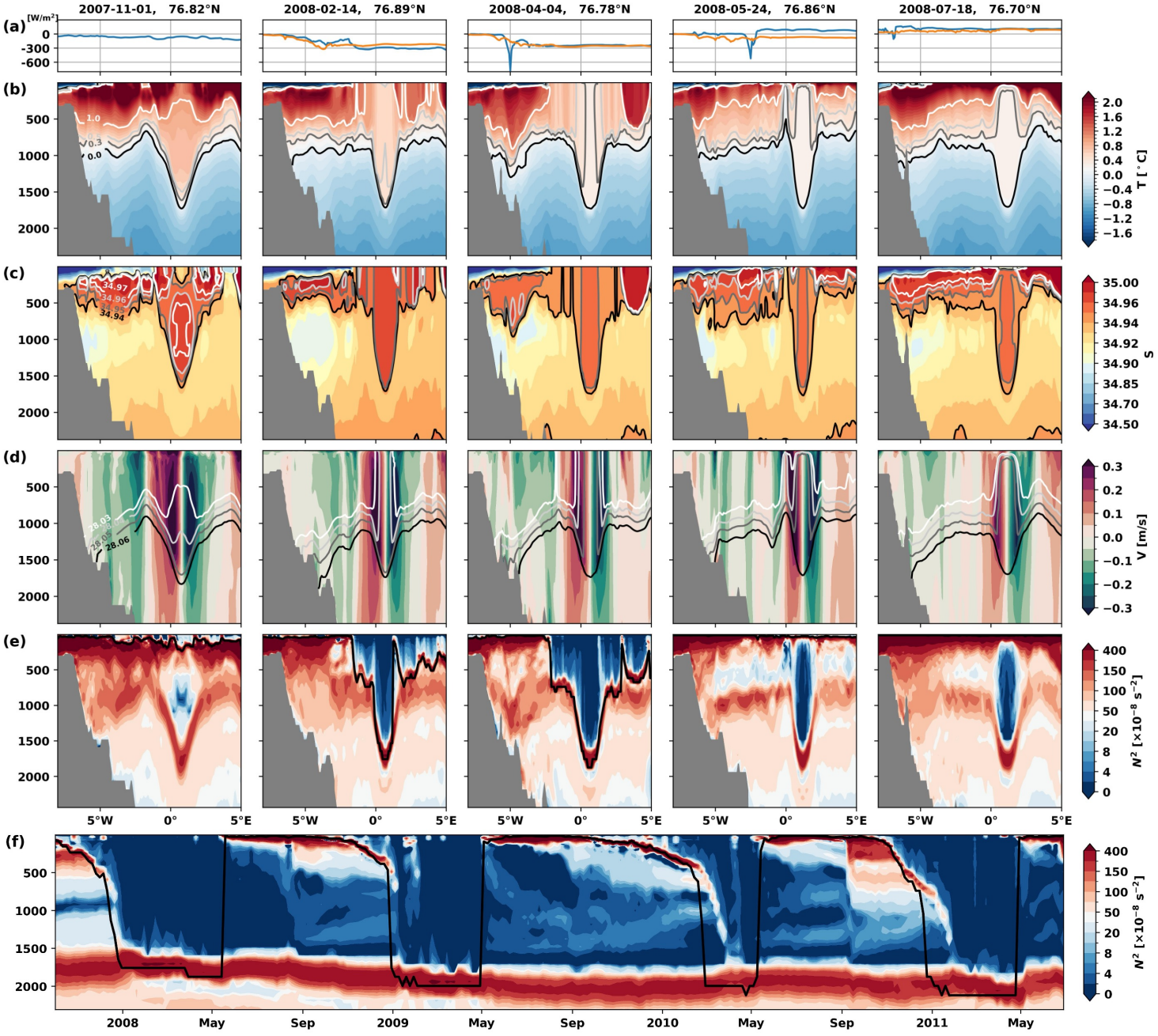

Figure 3. Zonal transects (8°W–5°E) across the tracked BB eddy center showing (a) net surface heat flux, (b) potential temperature, (c) salinity, (d) meridional velocity, and (e) N^2 for five representative dates in 2008 event. (f) N^2 in tracked eddy core from October 2007 to June 2011. The corresponding dates and latitudes are indicated at the top for panels (a-e), ice edge is indicated by cold, fresh surface water. In (a), the blue line shows the five-day mean net surface heat flux preceding each date, while the orange line shows the interval-mean between the current and previous dates. Panels (b–e) show instantaneous snapshots on the corresponding dates. White, light gray, dark gray, and black contours in (b–d) denote 1, 0.5, 0.3, and 0°C isotherms; 34.97, 34.96, 34.95, and 34.94 isohalines; and 28.03, 28.04, 28.05, and 28.06 kg m^{-3} isopycnals, respectively. In (e-f), black line denotes mixed-layer depth (MLD).

remnant. Once surface stratification is re-established, conventional MLD criteria fail to detect isolated mixed layers but convective lenses persist below the surface.

Restratification (column 5): During summer, surface heating leads to enhanced stratification of the upper ocean. Nevertheless, the eddy retains its characteristic upper-domed and lower-depressed isopycnal structure, with a weakly stratified rotating eddy core. Below the surface, this stage resembles the initial phase. Indeed, an analysis of the subsequent winter confirms the recurrence of this cycle (Figure S2) and demonstrates the longevity of the simulated BB eddy.

3.2.2 75°N Eddy

The simulated 75°N eddy is consistent with historical observations (Wadhams, 2005; Budéus & Ronski, 2009), standing out from other eddies by its deep vertical penetration, persistence, and distinct evolution (Figure 4). Given its similar evolution to the previously described eddy, we highlight its similarity to previous observations:

In April (column 3), the model reproduces a deep, vertically homogeneous water column with concave thermocline and halocline structures at the base of the 75°N eddy, in agreement with ship-based observations from April 2001 at 75°N (Wadhams et al., 2002). The upper 1200 m is strongly cooled and mixed, pushing the stratification maximum downward without reaching the bottom and forming a well-defined convective chimney. Compared to late February (column 2), the chimney remains quasi-stationary but becomes narrower, colder, and denser, indicating progressively localized homogenization over two months within the eddy core.

Prior to chimney formation, the tracked feature is an anticyclonic eddy undergoing progressive cooling and homogenization under moderate surface forcing (columns 1–2). It is already distinguished from the surrounding waters in October by its pronounced vertical extent and buoyant conical structure capped by warm, fresh surface water, which insulates the eddy interior from atmospheric fluxes. The eddy features an anticyclonically rotating, weakly stratified core with distinct temperature and salinity properties. Despite basin-scale cyclonic circulation gently uplifts interior layers, isopycnals denser than 28.04 kg m^{-3} remain depressed within the 75°N eddy. By late February, transient heat fluxes reaching up to -1000 W m^{-2} lift isopycnals toward the surface and re-ventilate Atlantic-origin waters near the ice edge, a feature recently observed (Våge et al., 2018). In contrast, the centrally located 75°N eddy experiences moderate but persistent heat loss since October, which preferentially erodes stratification within the eddy core. The cumulative winter heat loss substantially cools the upper ocean and produces a convective lens: a locally homogenized, cooling, and densifying water mass within the eddy.

Following the cessation of surface cooling, the chimney collapses and upper-ocean restratification begins (columns 4–5). The eddy is re-capped by warm, saline surface water, while retaining its characteristic upper-domed and lower-depressed isopycnals that define a postconvective eddy, a structure frequently observed after active wintertime convection (Gascard et al., 2002; Budéus et al., 2004). Consistently, zonal sections of temperature, salinity, density, and stability closely resemble those of the long-lived 75°N vortex depicted in Figure 2 of Budéus et al. (2004). During this stage, dense isopycnals (28.06–28.08 kg m^{-3}) are further displaced downward, submerging the eddy core. Within the eddy depth range, water properties become laterally mixed and weakly buoyant, consistent with the lateral spreading phase of classical open-ocean convection (Marshall & Schott, 1999). Owing to its longevity, this trapped, weakly stratified water provides memory that preconditions the eddy for renewed convection in subsequent winters when upper stratification is eroded (Figure S3).

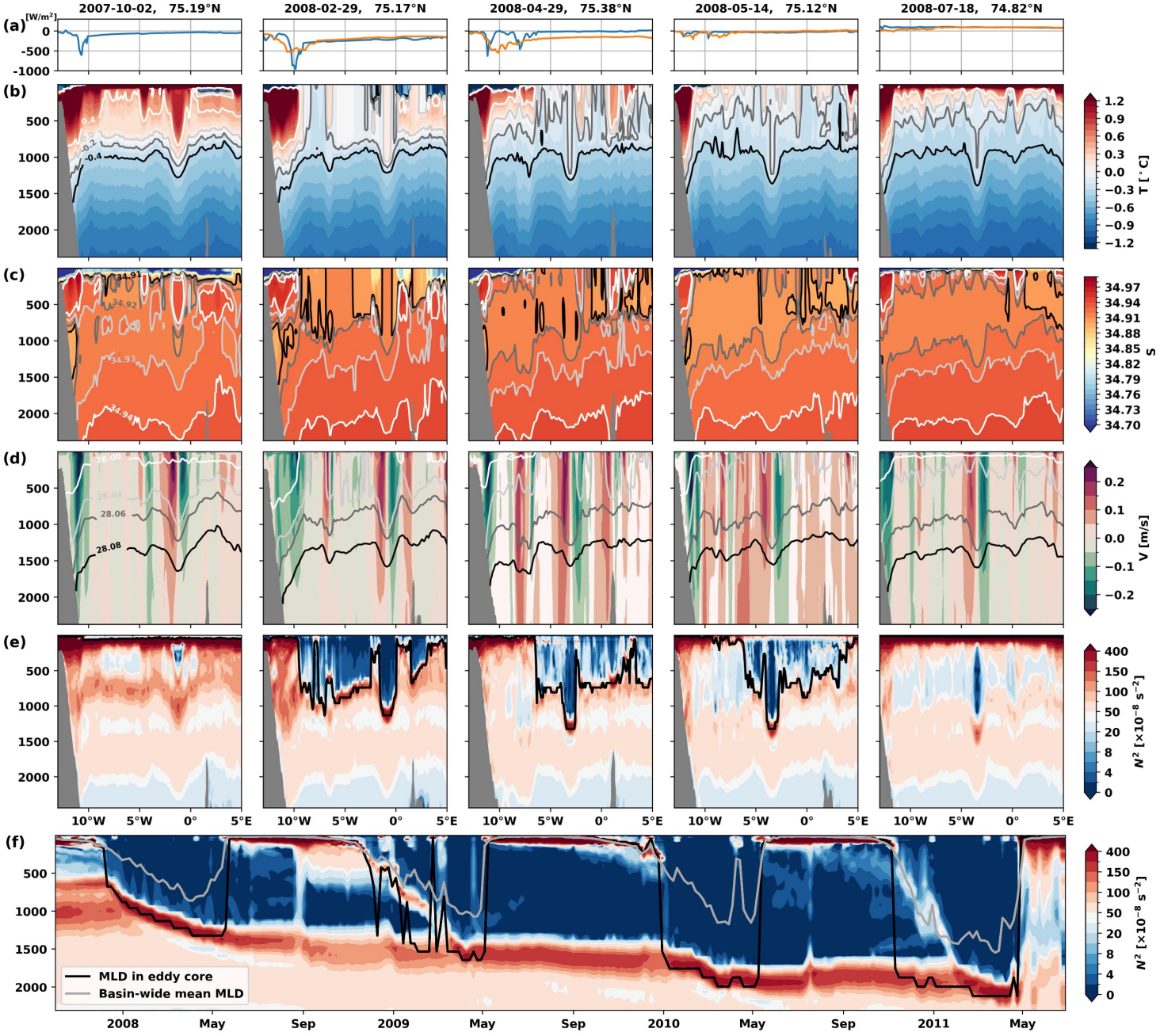

Figure 4. Same as Figure 3, but for the 75°N eddy. White, light gray, dark gray and black contours in panels (b-d) denote 0.4, 0, -0.2, -0.4 isotherms; 34.94, 34.93, 34.92, 34.91 isohalines; and 28.00, 28.04, 28.06, 28.08 kg m^{-3} isopycnals, respectively. In (f), mixed-layer depth (MLD) within tracked eddy core is compared with basin-mean MLD averaged over the Greenland Basin within the 3200 m isobath.

4 Discussion

4.1 On the longevity and isopycnal structure

The BB and 75°N eddies belong to the same family; both are long-lived vortices and exhibit dynamical consistency with previous observations in several key respects (Gascard et al., 2002; Budéus et al., 2004; Wadhams, 2005): (1) During winter, a homogeneous convective chimney forms within the eddy core and extends to great depth. The chimney experiences localized progressive cooling and densification, clearly distinguished from the surrounding waters, similar to the observed features in March 2001 (Wadhams et al., 2002). (2) Following active convection, upper-domed and lower-depressed structures develop and can persist through stepwise adjustment cycles. This persistence explains the similar 75°N transects frequently observed from spring through autumn (Gascard et al., 2002; Logemann, 2001; Budéus et al., 2004; Wadhams et al., 2004; Kasajima et al., 2006; Ronski & Budéus, 2006; Olsen et al., 2024). (3) The eddy core becomes isolated at depth, remains weakly stratified, and capped by surface stratification while a secondary mid-depth stratified layer is displaced downward. This structure is renewed through repeated cycles of wintertime erosion, atmospheric re-exposure, and postconvective adjustment.

Time series of the modeled N^2 and MLD in the eddy centers from 2007 to 2011 illustrate that such eddies are long-lived and undergo repeated "recharging" (Figure 3f, 4f). Stability indicated by N^2 exhibits repeated progressive deepening and homogenization during wintertime convection over multiple years, provided the eddy is not capped by stratified surface water or intermittently covered by sea ice. This process contributes to eddy longevity by repeatedly homogenizing and possibly re-energizing the core through surface forcing (Budéus et al., 2004). The MLD evolves accordingly as the eddy column progressively cools and densifies. Situated within topographic depressions and surrounded by the unstable currents and frequently advected eddies, these long-lived vortices undergo frequent merging and filament-absorption events. Such processes modify water-mass properties and likely sustain their persistence. In particular, anticyclonic eddies shed from the currents preferentially propagate toward topographic depression, a mechanism commonly believed to sustain long-lived vortices (Köhl, 2007; LaCasce et al., 2024).

Such anticyclonic eddies exhibit upper-domed and lower-depressed isopycnals, leading some studies to interpret these vortices conceptually as hetons, consisting of a cyclonic upper layer overlying an anticyclonic lower layer inferred from the implied geostrophic shear (Oliver et al., 2008). However, the model demonstrates that these eddies rotate anticyclonically throughout the water column, as also found by vessel mounted ADCP velocity measurements (Budéus et al., 2004). This indicates that the apparent reversal in isopycnal curvature does not correspond to a reversal in vorticity, but rather reflects the vertical redistribution of density following deep convection. The surrounding cyclonic flow may help sustain its upper-domed isopycnals by uplifting interior density surfaces. Dynamically, these eddies closely resemble mode-water eddies, characterized by an isolated, thick, weakly stratified core that lifts the upper pycnocline and depresses the lower pycnocline (McGillicuddy Jr, 2016).

4.2 On the role in convection

Convection behaves distinctly within long-lived eddies. Near the ice margin, convection is typically driven by episodic extreme heat loss associated with synoptic cold-air outbreaks (Papritz & Spengler, 2017; Terpstra et al., 2021). Despite its intensity, this forcing is short-lived and does not necessarily produce sustained mixed-layer deepening, as the underlying water can be rapidly advected away (Renfrew et al., 2021, 2023; Semper et al., 2025). In contrast, surface heat loss over the open ocean is comparatively moderate but persistent. Relative to nearby ambient waters, the eddy cores exhibit weaker stratification before winter, faster erosion of stratification, and deeper mixed-layer development under the same sustained wintertime forcing. The basin-scale cyclonic gyre

uplifts interior waters, favoring winter convection, while embedded long-lived anticyclonic eddies are localized reservoirs of weak stratification that facilitate earlier onset and prolonged convective mixing. This enhanced response reflects the preconditioning effect of the upper-domed isopycnal, which elevates interior waters even closer to the surface and increases their exposure to atmospheric forcing.

A notable but rarely discussed feature of Greenland Sea convection is the multi-year deepening of MLD during the 1990s and 2000s, linked to the basin-scale descent of the stratification maximum during the transition from Greenland Sea Deep Water to Greenland Sea Arctic Intermediate Water formation (Brakstad et al., 2019; Strehl et al., 2024) and captured by three moored profilers over 10 years (Svingen et al., 2023). We note that MLD evolution within long-lived eddies resembles that of the basin-wide background stratification, but is most pronounced in the eddy cores and weaker when averaged over the broader basin (Figure 4f). Given the mobility of long-lived eddies in the Greenland Basin, further investigation is needed to determine whether, and how, these anticyclones interact with basin-scale stratification changes.

The 75°N eddy becomes ambiguous to track after undergoing substantial decay and splitting during the winter of 2011 (Figure S4), whereas the BB eddy appears quasi-permanent. In the simulation, the 75°N eddy persists through four winters, a lifespan that is consistent with historical observations in 1997, 2001, 2002, 2003, 2005, and 2016 (Gascard et al., 2002; Logemann, 2001; Budéus et al., 2004; Kasajima et al., 2006; Ronski & Budéus, 2006; Olsen et al., 2024). To conclude, their longevity is accompanied by a combination of topographic trapping, eddy merging, and repeated wintertime convection that may re-energize the eddy. This persistence imparts multiyear memory to the coherent eddies, enabling them to act as localized reservoirs of weak stratification that preferentially host deep convection under moderate and sustained surface cooling.

Open Research Section

Argo floats (WMO IDs: 6900305, 6900609, 7900169, 7900170, 7900171, 7900172, 7900178) and drifters (WMO IDs: 6300931, 6300944) data used in this study is retrieved from the Argovis web application (Mills et al., 2025), `https://argovis.colorado.edu/`; Global Ocean Gridded L4 Sea Surface Heights And Derived Surface Geostrophic Velocity (CMEMS, 2025) is available on `https://data.marine.copernicus.eu/product/SEALEVEL_GLO_PHY_L4_MY_008_047/description`. SWOT L3 product (SWOT, 2023) is available on `https://www.aviso.altimetry.fr/en/data/products/sea-surface-height-products/global/swot-l3-ocean-products.html`. The observed sea ice extent is from Climate Data Record (Meier et al., 2024) via `https://noaadata.apps.nsidc.org/NOAA/G02202_V5/north/`. Model output used in this study is available on Zenodo (Jian, 2026).

Acknowledgments

D.J. acknowledges funding from the China Scholarship Council, the University of East Anglia (UEA), doctoral training support from the ARIES Doctoral Training Partnership. I.A.R. acknowledges partial support from the UK's Natural Environment Research Council (NERC) Grant (NE/N009754/1). The model simulation and post-processing were conducted on the High-Performance Computing Cluster supported by the Research and Specialist Computing Support service at UEA. We are grateful to the reviewers for their constructive comments.

Conflict of Interest

The authors declare no conflicts of interest relevant to this study.

References

Abot, L., Provost, C., & Poli, L. (2023). Recent Convection Decline in the Greenland Sea: Insights From the Mercator Ocean System Over 2008–2020. *Journal of Geophysical Research: Oceans*, *128*(6), e2022JC019320. doi: 10.1029/2022JC019320

Almeida, L., Kolodziejczyk, N., & Lique, C. (2023). Large Scale Salinity Anomaly Has Triggered the Recent Decline of Winter Convection in the Greenland Sea. *Geophysical Research Letters*, *50*(21), e2023GL104766. doi: 10.1029/2023GL104766

Bashmachnikov, I. L., Kozlov, I. E., Petrenko, L. A., Glok, N. I., & Wekerle, C. (2020). Eddies in the North Greenland Sea and Fram Strait From Satellite Altimetry, SAR and High-Resolution Model Data. *Journal of Geophysical Research: Oceans*, *125*(7), e2019JC015832. doi: 10.1029/2019JC015832

Brakstad, A., Gebbie, G., Våge, K., Jeansson, E., & Ólafsdóttir, S. R. (2023). Formation and pathways of dense water in the Nordic Seas based on a regional inversion. *Progress in Oceanography*, *212*, 102981. doi: 10.1016/j.pocean.2023.102981

Brakstad, A., Våge, K., Håvik, L., & Moore, G. W. K. (2019). Water Mass Transformation in the Greenland Sea during the Period 1986–2016. *Journal of Physical Oceanography*, *49*(1). doi: 10.1175/JPO-D-17-0273.1

Budéus, G., & Ronski, S. (2009). An integral view of the hydrographic development in the greenland sea over a decade. *The Open Oceanography Journal*, *3*, 8–39.

Budéus, G., Cisewski, B., Ronski, S., Dietrich, D., & Weitere, M. (2004). Structure and effects of a long lived vortex in the Greenland Sea. *Geophysical Research Letters*, *31*(5). doi: 10.1029/2003GL017983

CMEMS. (2025). *Global Ocean Gridded L4 Sea Surface Heights and Derived Variables Reprocessed 1993–Ongoing (Product ID: SEALEVEL_GLO_PHY_L4_MY_008_047) [Dataset].* E.U. Copernicus Marine Service Information (CMEMS), Marine Data Store (MDS). doi: 10.48670/moi-00148

Gascard, J.-C., Watson, A. J., Messias, M.-J., Olsson, K. A., Johannessen, T., & Simonsen, K. (2002). Long-lived vortices as a mode of deep ventilation in the Greenland Sea. *Nature*, *416*(6880), 525–527. doi: 10.1038/416525a

Håvik, L., Pickart, R. S., Våge, K., Torres, D., Thurnherr, A. M., Beszczynska-Möller, A., ... von Appen, W.-J. (2017). Evolution of the East Greenland Current from Fram Strait to Denmark Strait: Synoptic measurements from summer 2012. *Journal of Geophysical Research: Oceans*, *122*(3), 1974–1994. doi: 10.1002/2016JC012228

IOC, S., et al. (2010). The international thermodynamic equation of seawater–2010: Calculation and use of thermodynamic properties. *Intergovernmental Oceanographic Commission, UNESCO Manuals and Guides No*, *56*(203), 196.

Jensen, S., Andersen, O., Ludwigsen, C., Gonçalves-Araujo, R., & De Steur, L. (2025). Surface water and ocean topography (swot) observations unveil small mesoscale variability on the east greenland shelf. *Geophysical Research Letters*, *52*(21), e2025GL118573.

Jian, D. (2026). Mitgcm simulation for the manuscript "long-lived anticyclonic eddies facilitate convection in the greenland sea over multiple consecutive winters" submitted to grl (version v1.0.0) [dataset]. *Zenodo*. doi: 10.5281/zenodo.20003941

Jian, D., Zhai, X., Stevens, D. P., & Renfrew, I. A. (2026). Oceanic heat transport along the norwegian atlantic slope current and the role of eddies. *Journal of Geophysical Research: Oceans*, *131*(1), e2025JC022960. doi: 10.1029/2025JC022960

Kasajima, Y., Olsson, K. A., Johannessen, T., Messias, M.-J., Jeansson, E., Bellerby, R. G. J., & Skjelvan, I. (2006). A submesoscale coherent eddy in the Green-

land Sea in 2003. *Journal of Geophysical Research: Oceans*, *111*(C7). doi: 10.1029/2005JC003130

Köhl, A. (2007). Generation and Stability of a Quasi-Permanent Vortex in the Lofoten Basin. *Journal of Physical Oceanography*, *37*(11), 2637–2651. doi: 10.1175/2007JPO3694.1

LaCasce, J. H., Palóczy, A., & Trodahl, M. (2024). Vortices over bathymetry. *Journal of Fluid Mechanics*, *979*, A32. doi: 10.1017/jfm.2023.1084

Large, W. G., McWilliams, J. C., & Doney, S. C. (1994). Oceanic vertical mixing: A review and a model with a nonlocal boundary layer parameterization. *Reviews of Geophysics*, *32*(4), 363–403. doi: 10.1029/94RG01872

Logemann, K. (2001). *Report of cruise # 21-2001 of rv LANCE: Investigations of the hydrography in the greenland sea, september 2001, tromsø–longyearbyen, 7 september–2 october 2001* (Tech. Rep.). Institut für Meereskunde, Universität Hamburg. Retrieved from `https://www.ifm.uni-hamburg.de/workareas/experimental/berichte/lance21_2001.pdf`

Marshall, J., Adcroft, A., Hill, C., Perelman, L., & Heisey, C. (1997). A finite-volume, incompressible Navier Stokes model for studies of the ocean on parallel computers. *Journal of Geophysical Research: Oceans*, *102*(C3), 5753–5766. doi: 10.1029/96JC02775

Marshall, J., & Schott, F. (1999). Open-ocean convection: Observations, theory, and models. *Reviews of Geophysics*, *37*(1), 1–64. doi: 10.1029/98RG02739

McGillicuddy Jr, D. J. (2016). Mechanisms of physical-biological-biogeochemical interaction at the oceanic mesoscale. *Annual Review of Marine Science*, *8*(1), 125–159. doi: 10.1146/annurev-marine-010814-015606

Meier, W., Fetterer, F., Windnagel, A., Stewart, J. S., & Stafford, T. (2024). *NOAA/NSIDC Climate Data Record of Passive Microwave Sea Ice Concentration. (G02202, Version 5). [Dataset].* Boulder, Colorado USA. National Snow and Ice Data Center. doi: 10.7265/RJZB-PF78

Mills, B. K.-A., Giglio, D., Scanderbeg, M., Purkey, S., & Merchant, L. (2025). Argovis: Building a fair ocean data service. *Journal of Atmospheric and Oceanic Technology*, *42*(11), 1567–1581. doi: 10.1175/JTECH-D-24-0160.1

Morozov, E. A., & Kozlov, I. E. (2023). Eddies in the arctic ocean revealed from modis optical imagery. *Remote Sensing*, *15*(6), 1608. doi: 10.3390/rs15061608

Nurser, A. J. G., & Bacon, S. (2014). The Rossby radius in the Arctic Ocean. *Ocean Science*, *10*(6), 967–975. doi: 10.5194/os-10-967-2014

Oliver, K., Eldevik, T., Stevens, D., & Watson, A. (2008). A greenland sea perspective on the dynamics of postconvective eddies. *Journal of Physical Oceanography*, *38*(12), 2755–2771. doi: 10.1175/2008JPO3844.1

Olsen, A., Rajasakaren, B., Jeansson, E., Lauvset, S. K., Omar, A. M., & Becker, M. (2024). In the wake of deeper convection: Nonsteady state anthropogenic carbon in the greenland sea. *Journal of Geophysical Research: Oceans*, *129*(6), e2023JC020462. doi: 10.1029/2023JC020462

Papritz, L., & Spengler, T. (2017). A lagrangian climatology of wintertime cold air outbreaks in the irminger and nordic seas and their role in shaping air–sea heat fluxes. *Journal of Climate*, *30*(8), 2717–2737. doi: 10.1175/JCLI-D-16-0605.1

Quadfasel, D., & Meincke, J. (1987). Note on the thermal structure of the greenland sea gyres. *Deep sea research Part A. Oceanographic Research Papers*, *34*(11), 1883–1888. doi: 10.1016/0198-0149(87)90061-6

Renfrew, I. A., Barrell, C., Elvidge, A. D., Brooke, J. K., Duscha, C., King, J. C., ... Weiss, A. (2021). An evaluation of surface meteorology and fluxes over the Iceland and Greenland Seas in ERA5 reanalysis: The impact of sea ice distribution. *Quarterly Journal of the Royal Meteorological Society*, *147*(734), 691–712. doi: 10.1002/qj.3941

Renfrew, I. A., Huang, J., Semper, S., Barrell, C., Terpstra, A., Pickart, R. S., ... Weiss, A. (2023). Coupled atmosphere–ocean observations of a cold-air outbreak and its impact on the Iceland Sea. *Quarterly Journal of the Royal Meteorological Society*, *149*(751), 472–493. doi: 10.1002/qj.4418

Ronski, S., & Budéus, G. (2006). Vertical structure reveals eddy lifetime in the greenland sea. *Geophysical research letters*, *33*(11). doi: 10.1029/2006GL026045

Semper, S., Våge, K., Fer, I., Latuta, L., & Skjelsvik, S. (2025). Formation and circulation of dense water from a two-year moored record in the northwestern iceland sea. *Journal of Geophysical Research: Oceans*, *130*(5), e2024JC021691. doi: 10.1029/2024JC021691

Strehl, A.-M., Våge, K., Smedsrud, L. H., & Barreyre, T. (2024). A 70-year perspective on water-mass transformation in the Greenland Sea: From thermobaric to thermal convection. *Progress in Oceanography*, *227*, 103304. doi: 10.1016/j.pocean.2024.103304

Svingen, K., Brakstad, A., Våge, K., Appen, W.-J. v., & Papritz, L. (2023). The Impact of Cold-Air Outbreaks and Oceanic Lateral Fluxes on Dense-Water Formation in the Greenland Sea from a 10-Year Moored Record (1999–2009). *Journal of Physical Oceanography*, *53*(6). doi: 10.1175/JPO-D-22-0160.1

SWOT. (2023). *SWOT Level-3 SSH Expert (v3.0) [Dataset].* CNES. doi: 10.24400/527896/A01-2023.018

Talley, L. D. (2011). *Descriptive physical oceanography: an introduction.* Academic press.

Terpstra, A., Renfrew, I. A., & Sergeev, D. E. (2021). Characteristics of cold-air outbreak events and associated polar mesoscale cyclogenesis over the north atlantic region. *Journal of Climate*, *34*(11), 4567–4584. doi: 10.1175/JCLI-D-20-0595.1

Våge, K., Moore, G. W. K., Jónsson, S., & Valdimarsson, H. (2015). Water mass transformation in the iceland sea. *Deep Sea Research Part I: Oceanographic Research Papers*, *101*, 98–109. doi: 10.1016/j.dsr.2015.04.001

Våge, K., Pickart, R. S., Thierry, V., Reverdin, G., Lee, C. M., Petrie, B., ... Ribergaard, M. H. (2009). Surprising return of deep convection to the subpolar north atlantic ocean in winter 2007–2008. *Nature Geoscience*, *2*(1), 67–72. doi: 10.1038/NGEO382

Våge, K., Papritz, L., Håvik, L., Spall, M. A., & Moore, G. W. K. (2018). Ocean convection linked to the recent ice edge retreat along east Greenland. *Nature Communications*, *9*(1). doi: 10.1038/s41467-018-03468-6

Wadhams, P. (2005). Convective chimneys in the greenland sea: A review of recent observations. *Oceanography and Marine Biology: An Annual Review*, *42*, 1–28.

Wadhams, P., Budéus, G., Wilkinson, J. P., Løyning, T., & Pavlov, V. (2004). The multi-year development of long-lived convective chimneys in the Greenland Sea. *Geophysical Research Letters*, *31*(6). doi: 10.1029/2003GL019017

Wadhams, P., Holfort, J., Hansen, E., & Wilkinson, J. P. (2002). A deep convective chimney in the winter greenland sea. *Geophysical Research Letters*, *29*(10), 76–1–76–4. doi: 10.1029/2001GL014306